

ORIGINAL ARTICLE

Open Access



Effect of pyrolysis temperature on composition, carbon fraction and abiotic stability of straw biochars: correlation and quantitative analysis

Xiaoxiao Zhang, Xueqi Yang, Xiangru Yuan, Sicong Tian, Xinlei Wang, Hehu Zhang and Lujia Han*

Abstract

Biochar provides an important pathway for the global response to climate change. The abiotic stability of biochar is important for its application in carbon capture and sequestration. To systematically illustrate the effects of pyrolysis temperature on composition, carbon fraction and abiotic stability of straw biochar, four kinds of straw biochars were prepared at pyrolysis temperatures of 300 °C, 400 °C, 500 °C, and 600 °C, respectively. The ultimate and proximate compositions, different carbon fractions and abiotic stability of prepared biochar were characterized, and their qualitative and quantitative relationships were established by Kendall correlation analysis, factor analysis and different regression analysis methods. Results showed that pyrolysis temperature influenced compositions and carbon fractions directly, which affected the abiotic stability of biochar ($p < 0.01$). The higher the pyrolysis temperature (up to 500 °C), the higher the abiotic stability of biochar. The different abiotic stability indicators, including thermal stability (ratios of volatile matter and fixed carbon, hydrogen and organic carbon, oxygen and organic carbon, and thermal stability index R_{50}), dissolution stability and chemical oxidation-resistant stability of biochar, all followed exponential functions with pyrolysis temperature. Unitary and binary linear regression equations among compositions, carbon fractions and the abiotic stability evaluation indicators were established. We hope that the results are scientifically valuable for a better understanding of the inherent properties of straw biochar, and thus help simplify the screening of appropriate indicators for evaluating the properties and abiotic stability of biochar.

Highlights

- Four kinds of straw biochars were produced at different pyrolysis temperatures.
- Composition, carbon fraction and abiotic stability of biochars were characterized.
- Quantitative effects of pyrolysis temperature on biochars were established.
- Abiotic stability evaluation indicators of biochar were exponential functions of pyrolysis temperature.
- Significant relationships among abiotic stability evaluation indicators were shown in detail.

Keywords: Straw biochar, Abiotic stability, Pyrolysis temperature, Quantitative relationship, Carbon fraction, Chemical composition

*Correspondence: hanlj@cau.edu.cn

College of Engineering, China Agricultural University, Beijing 100083, China

Graphical Abstract

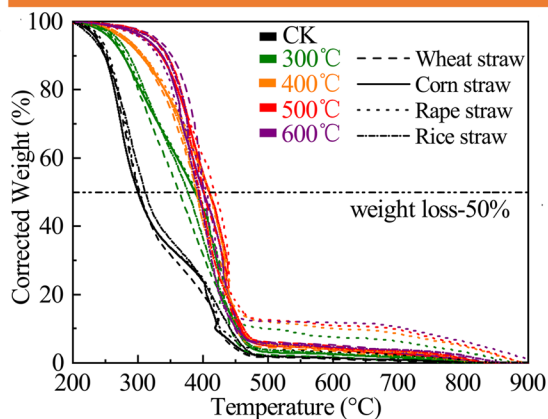
Straw biochars

Pyrolysis temperature

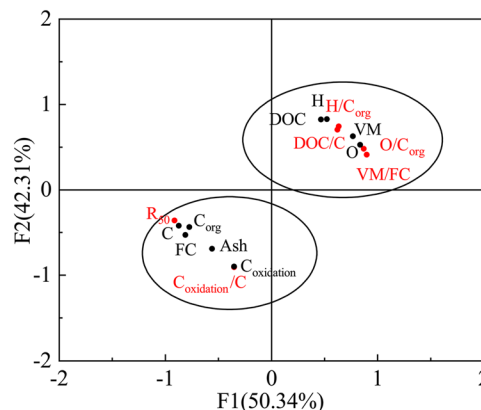
300 °C, 400 °C, 500 °C, 600 °C



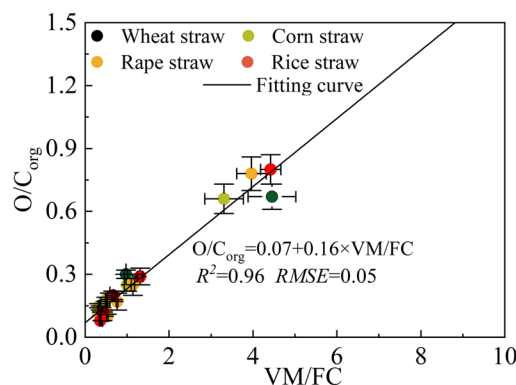
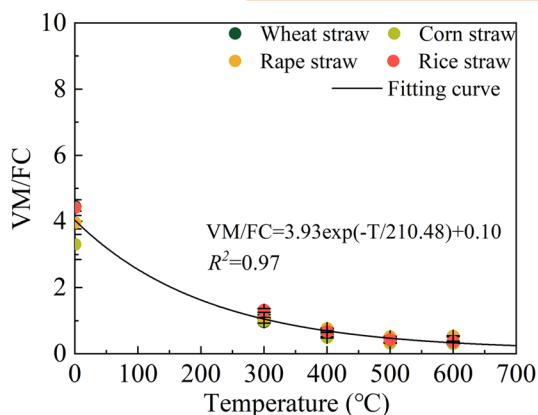
The corrected temperature programmed oxidation curves



Factor analysis of composition, carbon fraction and abiotic stability



Correlation and quantitative analysis



1 Introduction

Biochar is a kind of porous and carbon-rich organic material derived from the pyrolysis of biomass, including all kinds of crop straws, forestry residues, livestock manure and other wastes, under relatively low temperatures (300–700 °C) and restricted oxygen conditions. Applying biochar to pollution abatement on soil or water (Kim et al. 2021; Zhang et al. 2019), carbon (C) emission reduction (Qian et al. 2015; Woolf et al. 2010),

also C capture and sequestration (Singh et al. 2019) has exhibited a great development potential.

The whole process from production to utilization in the biochar-soil system (biochar production and its storage in soil) is regarded as a typical carbon-negative emission activity (Lehmann 2007). Biochar returning to the field is beneficial to agricultural production and climate change mitigation, which has attracted more and more attention in the international community of climate change.

It is estimated that biochar can offer carbon dioxide (CO₂) removal potential of 0.3 to 2 Gt per year (Hepburn et al. 2019). The world-renowned scientific journals such as *Nature* and *Science* have published feature articles emphasizing the combination of plant carbon fixation and biochar production for filed return, calling for increased research on the environmental behavior and environmental impact of biochar-soil system (Paustian et al. 2016; Sohi 2012), to provide important support for global climate change.

The stability of biochar, such as the persistence of biochar in the environment, can reflect the resistance to biotic and abiotic decomposition. The biotic stability of biochar is mainly affected by microorganism-induced oxidative decomposition process (Ameloot et al. 2013). And the abiotic stability of biochar is mainly affected by dissolution (Lian and Xing 2017) and oxidation (chemical oxidations, oxygen and temperature) (Wang et al. 2017) of biochar in the environment. Microorganisms in soil can cause the biotic consumption of C fixed by biochar, however, the abiotic factors can influence the rate of biochar decomposition, leading overestimating the potential of C sequestration (Yu et al. 2020).

Previous studies have shown that the abiotic stability of biochar is closely related to its composition properties and environmental applications (De la Rosa et al. 2018; Leng et al. 2019). Pyrolysis temperature and feedstock have a direct influence on the composition properties of biochar (Das et al. 2021; Hassan et al. 2020; Kim et al. 2020; Wu et al. 2022; Xu et al. 2021; Zhang et al. 2020). Biochar applied into soil will be affected by several abiotic factors, such as rainfall (Wang et al. 2022), temperature changes (Liu and Chen 2022), and environmental oxidation (Wang et al. 2021a). For example, rainfall can cause biochar to release soluble organic matter or mineral components by dissolution (Wang et al. 2021b). Dissolved organic carbon (DOC) is an important component of soluble organic matter, which will flow into the water environment through surface runoff (Jaffe et al. 2013) or infiltrate into the soil and then be used by microorganisms (Quan et al. 2020), decreasing the capacity of C sequestration. Furthermore, the surface properties of biochar will undergo chemical oxidation under soil oxides or light conditions, which will make the C in biochar thermodynamically unstable under aerobic conditions (Wang et al. 2021a).

The abiotic stability of biochar has been evaluated by extensive studies (Liu et al. 2020a, 2020b; Pariyar et al. 2020; Wei et al. 2019; Zornoza et al. 2016). Most studies only focused on the single or multi-composition changes related to the above influencing factors, however, universal methods that can directly or indirectly evaluate the abiotic stability of biochar are missing (Leng and Huang

2018; Leng et al. 2019), causing difficulties in the practical evaluation of biochar stability. For instance, the ratio of volatile matter (VM) to fixed carbon (FC) (Aller et al. 2017) and the thermal stability index R_{50} (calculated as the ratio of temperatures at which half weight loss occurs during calcination of biochar and graphite, respectively) (Gómez et al. 2016) can be used to evaluate the thermal stability of biochar. International Biochar Initiative (IBI) and European Biochar Foundation (EBC) recommended using the atomic ratios of hydrogen (H) and organic carbon (C_{org}) or oxygen (O) and C_{org} to assess the stability of the carbon structure in biochar (Leng et al. 2019). DOC was used to evaluate the dissolution stability of biochar (Han et al. 2020); the chemical oxidation-resistant carbon (C_{oxidation}) could reflect the oxidation-resistance of biochar (Liu et al. 2020a, b), and the ratio of C_{oxidation} and C can reflect the chemical oxidation-resistant stability of biochar (Calvelo-Pereira et al. 2011).

Given the above mentioned examples, the abiotic stability of biochar is not only affected by feedstocks, process parameters, and composition characteristics, but is also closely related to the methods for stability evaluation. Therefore, four kinds of straws (wheat straw, corn straw, rape straw and rice straw) were used because of their large production and wide distribution. The objective of this study is to systematically illustrate the effects of pyrolysis temperature on composition, carbon fraction and the abiotic stability of straw biochar, and to establish the relationship between pyrolysis temperature, composition, carbon fraction and abiotic stability of straw biochar. The results are expected to be valuable for a scientific comprehension of the inherent properties of straw biochar, and thus help simplify the screening of appropriate indicators for evaluating the properties and abiotic stability of biochar.

2 Materials and methods

2.1 Biochar samples

Four kinds of straws (wheat straw, corn straw, rape straw, and rice straw) were used to produce biochar, and the detailed information about the biochar preparation was presented in author's previous research (Zhang et al. 2020). In brief, the feedstocks were crushed and dried, and then pyrolyzed in a tube furnace (GSL-1100X, Hefei Kejing Materials Technology Co. Ltd., China) under nitrogen (N₂) atmosphere (all straw samples without pyrolysis treatment were marked as CK). Since 300–600°C was an important temperature range for weight loss of straw (Zhang et al. 2020), four pyrolysis temperatures, 300°C, 400°C, 500°C, and 600°C were chosen for biochar preparation. The heating rate was 10°C/min and the pyrolysis process was held for 1 h at the final temperature.

2.2 Lab analysis of biochar characteristics

The elemental composition of straw feedstocks and biochar samples were analyzed by the elemental analyzer (Vario Macro Elementar, Germany).

The proximate composition was determined by a thermogravimetric analyzer (SDTQ600, TA Instruments, USA) using the method described in ref. (Crombie et al. 2013). The sample placed into the crucible was heated to 105 °C under N₂ for 10 min to obtain the moisture (MC) content, and then was heated at 25 °C/min to 900 °C where kept for a further 10 min to remove VM. Introduced the air into test system, the sample was combusted at 750 °C (the test temperature was set according to ASTM D5142–09) for 15 min, and the residual weight was ash content. The content of FC was calculated by difference (FC = 100-MC-VM-ash).

C_{org} was measured by total organic C analyzer (Elemental Vario TOC select, Germany). The sample was weighted into a silver boat and acidified using 1 M HCl solution; the acidified sample was dried at 100 °C for 1 h to remove inorganic C such as carbonate in biochar, and then were packed for analysis (Enders et al. 2012).

DOC was also determined by total organic C analyzer (Elemental Vario TOC select, Germany). The sample and deionized water were mixed at 1:20 (wt/v) and after shaking (150 rpm) for 2 hours, the treated sample was centrifuged at 10000 rpm for 10 min (Wu et al. 2019). Then, the filtrate used for final DOC analysis was obtained by supernatants through a 0.45 μm filter.

Potassium dichromate (K₂Cr₂O₇) has strong oxidation ability which can be used to determine carbon components that are not easy to decompose and oxidate potentially decomposable carbon structures (Calvelo-Pereira et al. 2011). The K₂Cr₂O₇ oxidation method was used for C_{oxidation} determination. The sample containing 0.1 g C (±0.0001 g) was weighted into a 50 ml centrifuge tube with 40 ml of 0.1 M K₂Cr₂O₇/2 M H₂SO₄ solution, and the chemical oxidation was performed at 55 °C for heating for 60 h (Yang et al. 2018). In order to ensure complete reaction, the oxidation solution was replaced for once after 30 h-reaction during the oxidation process. After the test, the solid phase was separated by centrifugation and then weighted after drying. The C content remained in solid phase was determined by the elemental analyzer (Vario Macro Elementar, Germany). The content of C_{oxidation} in sample was calculated as follows:

$$C_{oxidation}(\%) = (C_{after} \times W_{after}) / W_{before} \quad (1)$$

Where W_{before} and W_{after} were the mass (g) of the sample before and after oxidation, and C_{after} was the C content (%) of the sample after oxidation.

The temperature programmed oxidation (TPO) curves of samples, were measured by a thermogravimetric

analyzer (SDTQ600, TA Instruments, USA). Samples were placed in an aluminum crucible and heated to 1000 °C at a heating rate of 10 °C/min under air atmosphere. Then, the TPO curves were corrected following the method described in previous study (Harvey et al. 2012).

2.3 Calculation for the abiotic stability evaluation of biochar

VM/FC and atomic ratios (H/C_{org} and O/C_{org}) were calculated from the results of chemical analysis to evaluate the thermal stability of straw biochar.

R_{50} is also used for the evaluation of thermal stability. It was calculated as follows (Harvey et al. 2012):

$$R_{50} = T_{50x} / T_{50 \text{ graphite}} \quad (2)$$

Where, T_{50x} and $T_{50 \text{ graphite}}$ were the temperature (°C) of biochar and graphite where the mass loss was 50%. T_{50x} was obtained from the corrected TPO curves of samples, and $T_{50 \text{ graphite}}$ was 886 °C, which was taken from Harvey et al. (2012).

The dissolution stability was calculated by the percentage of DOC content in C content, expressed as DOC/C (%).

The oxidation resistant stability was calculated by the percentage of C_{oxidation} content in C content expressed as C_{oxidation}/C (%).

All tests were replicated three times.

2.4 Statistical analysis

A one-way analysis of variance (ANOVA) and Kendall correlation analysis were conducted using the software SPSS (IBM SPSS statistics 25), and the Turkey's HSD post-hoc tests ($p < 0.01$) (Jing et al. 2022) were used to identify significant differences among different biochars. All characteristics of samples were analyzed by SPSS using the factor analysis. Unitary and binary regression methods were performed with the software Origin (Origin lab 2018) and the correlation coefficient (R^2) was chosen to evaluate the goodness of fit.

3 Results and discussion

3.1 Effects of pyrolysis temperature on biochar composition and carbon fraction

The composition and carbon fraction related to abiotic stability of four kinds of straw feedstocks and their corresponding biochars at different pyrolysis temperatures are shown in Table 1.

Table 1 shows that the feedstock had no significant influence on H, FC, VM and C_{oxidation} ($p \geq 0.01$), but had a significant influence on C, DOC, C_{org} and ash ($p < 0.01$). Wheat straw had the highest content of C_{org}. Corn straw and rape straw had the highest content of C

Table 1 Ultimate analysis, proximate analysis and carbon fractions of straw biochars produced at different pyrolysis temperatures

Sample	Pyrolysis temperature(°C)	C (wt%) ¹	H (wt%) ¹	O (wt%) ¹	VM (wt%)	Ash (wt%)	FC (%)	C _{org} (%)	DOC (%)	C _{oxidation} (%)	
Wheat straw	CK	43.53 ± 0.19 ^{ab}	3.56 ± 0.25 ^{ea}	42.53	72.49 ± 2.11 ^{da}	7.44 ± 0.59 ^{ab}	16.29 ± 2.03 ^{aA}	47.61 ± 0.46 ^{ac}	2.32 ± 0.07 ^{db}	0.15 ± 0.13 ^{baA}	
	300	61.48 ± 0.43 ^{bb}	2.73 ± 0.07 ^{da}	19.61	39.73 ± 1.26 ^{ca}	15.38 ± 2.37 ^{ba}	41.02 ± 1.27 ^{bb}	49.01 ± 1.10 ^{abAb}	1.48 ± 0.03 ^{cb}	0.59 ± 0.51 ^{baA}	
	400	64.18 ± 0.37 ^b	1.78 ± 0.03 ^b	13.93	28.35 ± 2.26 ^{baB}	18.05 ± 1.75 ^{ba}	47.79 ± 2.28 ^{caB}	55.09 ± 2.16 ^{caB}	0.75 ± 0.01 ^{ba}	36.68 ± 0.64 ^{bd}	
	500	67.39 ± 0.32 ^c	1.01 ± 0.06 ^{bc}	7.35	20.19 ± 0.33 ^{aA}	24.91 ± 1.08 ^{cb}	49.16 ± 0.59 ^{caB}	54.24 ± 2.34 ^{baB}	0.10 ± 0.00 ^{aA}	61.17 ± 0.72 ^{cc}	
	600	65.34 ± 0.53 ^{db}	0.52 ± 0.03 ^{ab}	10.77	18.77 ± 0.59 ^{aA}	25.37 ± 1.08 ^{cb}	50.32 ± 0.89 ^{cb}	56.67 ± 1.75 ^{ca}	0.07 ± 0.00 ^{aA}	62.92 ± 1.50 ^{cc}	
	CK	44.53 ± 0.31 ^{ac}	5.31 ± 0.2 ^{eb}	41.18	70.96 ± 2.76 ^{da}	3.63 ± 0.68 ^{aA}	21.43 ± 2.83 ^{aA}	46.61 ± 1.37 ^{abC}	3.31 ± 0.21 ^{dc}	-	-
Corn straw	300	61.20 ± 0.43 ^{bb}	3.86 ± 0.09 ^{db}	17.39	40.50 ± 1.95 ^{caB}	13.84 ± 1.65 ^{ba}	40.38 ± 2.09 ^{bb}	52.50 ± 1.33 ^{bbC}	2.06 ± 0.04 ^{cc}	0.45 ± 0.08 ^{baA}	
	400	63.36 ± 0.70 ^{cb}	1.96 ± 0.02 ^b	13.46	25.81 ± 1.01 ^{ba}	17.26 ± 2.50 ^{ba}	51.11 ± 1.11 ^{cb}	56.85 ± 1.52 ^{bcAb}	0.96 ± 0.03 ^{bb}	24.12 ± 0.30 ^{bb}	
	500	65.08 ± 0.59 ^{db}	0.77 ± 0.04 ^{bb}	11.36	19.04 ± 0.41 ^{aA}	17.59 ± 1.63 ^{ba}	57.67 ± 0.36 ^{dc}	56.90 ± 0.82 ^{bcB}	0.16 ± 0.01 ^{ab}	56.82 ± 0.67 ^{cb}	
	600	67.48 ± 0.64 ^{cc}	0.18 ± 0.01 ^{aA}	8.98	17.59 ± 0.42 ^{aA}	19.93 ± 2.32 ^{ba}	56.29 ± 0.49 ^{dc}	58.54 ± 1.75 ^{ca}	0.06 ± 0.01 ^{aA}	58.13 ± 0.82 ^{caB}	
	CK	44.62 ± 0.19 ^{ac}	4.89 ± 0.05 ^{eb}	42.34	72.54 ± 1.64 ^{da}	4.44 ± 1.13 ^{abB}	18.30 ± 1.58 ^{aA}	40.75 ± 2.34 ^{abB}	1.65 ± 0.05 ^{ca}	-	-
	300	61.80 ± 0.18 ^{bb}	3.54 ± 0.2 ^{db}	17.95	43.56 ± 1.07 ^{ca}	13.97 ± 2.51 ^{ba}	38.26 ± 0.82 ^{bb}	54.59 ± 0.79 ^{bc}	2.89 ± 0.10 ^{db}	-	-
Rape straw	400	63.74 ± 0.45 ^{cb}	1.91 ± 0.2 ^{cb}	13.48	32.48 ± 0.73 ^{bb}	18.49 ± 1.83 ^{bcA}	42.83 ± 0.75 ^{ca}	58.86 ± 1.41 ^{bb}	1.39 ± 0.01 ^{bc}	31.45 ± 0.52 ^{ac}	
	500	66.96 ± 0.33 ^{dc}	0.87 ± 0.05 ^{bbc}	9.46	25.66 ± 0.89 ^{ab}	18.68 ± 2.00 ^{bcA}	49.85 ± 0.78 ^{eb}	57.66 ± 1.12 ^{bb}	0.17 ± 0.00 ^{ab}	53.59 ± 1.16 ^{bb}	
	600	67.85 ± 0.72 ^{dc}	0.18 ± 0.02 ^{aA}	7.89	24.53 ± 1.05 ^{ab}	22.13 ± 1.00 ^{caB}	46.65 ± 0.94 ^{aA}	59.60 ± 0.56 ^{ba}	0.07 ± 0.00 ^{aA}	59.96 ± 0.51 ^{cbC}	
	CK	42.12 ± 0.10 ^{pa}	4.16 ± 0.11 ^{ea}	41.22	69.44 ± 1.06 ^{da}	10.76 ± 1.08 ^{bc}	15.71 ± 0.83 ^{aA}	38.77 ± 1.91 ^{aA}	3.63 ± 0.14 ^{dc}	0.56 ± 0.07 ^{ab}	
	300	56.49 ± 0.20 ^{pa}	2.95 ± 0.13 ^{ca}	17.73	43.61 ± 1.13 ^{ca}	18.93 ± 0.90 ^{ba}	33.27 ± 1.13 ^{ba}	45.31 ± 1.45 ^{ba}	1.21 ± 0.07 ^{ca}	1.14 ± 0.10 ^{pa}	
	400	56.41 ± 0.07 ^{pa}	1.35 ± 0.10 ^{da}	13.71	28.76 ± 1.12 ^{baB}	23.29 ± 0.98 ^{ca}	42.85 ± 1.01 ^{ca}	51.76 ± 0.92 ^{cdA}	0.77 ± 0.01 ^{ba}	15.65 ± 0.61 ^{ba}	
500	59.59 ± 0.49 ^{ca}	0.47 ± 0.02 ^{ba}	8.27	20.25 ± 0.11 ^{aA}	27.13 ± 2.02 ^{caB}	47.79 ± 0.12 ^{da}	50.77 ± 0.61 ^{ca}	0.11 ± 0.00 ^{aA}	49.34 ± 1.06 ^{ca}		
	600	61.30 ± 0.29 ^{pa}	0.12 ± 0.02 ^{aA}	5.71	17.13 ± 0.99 ^{aA}	30.53 ± 0.66 ^{dc}	47.14 ± 1.10 ^{da}	56.34 ± 1.77 ^{da}	0.06 ± 0.00 ^{aA}	53.69 ± 1.75 ^{da}	

¹ The C, H, and O data were cited from Zhang et al. (2020); Different letters a, b, c, and d (A, B, C, and D) in the same column (line) show statistical differences ($p < 0.01$)

Table 2 Effects of pyrolysis temperature on the abiotic stability evaluation indicators of different straw biochars

Sample	Pyrolysis temperature(°C)	VM/FC	H/C _{org}	O/C _{org}	R ₅₀	DOC/C(%)	C _{oxidation} /C(%)
Wheat straw	CK	4.45 ± 0.57 ^{eA}	0.90 ± 0.07 ^{eA}	0.67 ± 0.06 ^{dA}	0.34 ± 0.00 ^{9A}	5.33 ± 0.16 ^{8B}	0.34 ± 0.30 ^{9A}
	300	0.97 ± 0.04 ^{dA}	0.67 ± 0.01 ^{dA}	0.30 ± 0.02 ^{CA}	0.42 ± 0.00 ^{9A}	2.41 ± 0.05 ^{dA}	0.96 ± 0.83 ^{9A}
	400	0.59 ± 0.06 ^{cAB}	0.39 ± 0.01 ^{cB}	0.19 ± 0.02 ^{BA}	0.44 ± 0.00 ^{CA}	1.17 ± 0.02 ^{CA}	57.15 ± 1.05 ^{8D}
	500	0.41 ± 0.01 ^{bB}	0.22 ± 0.01 ^{BC}	0.10 ± 0.02 ^{AA}	0.45 ± 0.00 ^{dB}	0.15 ± 0.00 ^{9A}	90.77 ± 1.15 ^{5C}
	600	0.37 ± 0.01 ^{aB}	0.11 ± 0.01 ^{aB}	0.14 ± 0.01 ^{abA}	0.45 ± 0.00 ^{dB}	0.11 ± 0.00 ^{9A}	96.30 ± 2.42 ^{8B}
Corn straw	CK	3.31 ± 0.46 ^{eA}	1.37 ± 0.10 ^{EB}	0.66 ± 0.07 ^{9A}	0.34 ± 0.00 ^{9A}	7.43 ± 0.47 ^{5C}	–
	300	1.00 ± 0.07 ^{dAB}	0.88 ± 0.01 ^{dC}	0.25 ± 0.03 ^{CA}	0.44 ± 0.00 ^{9C}	3.36 ± 0.07 ^{8B}	0.74 ± 0.13 ^{9A}
	400	0.50 ± 0.02 ^{CA}	0.41 ± 0.01 ^{cB}	0.18 ± 0.01 ^{bCA}	0.46 ± 0.00 ^{9B}	1.52 ± 0.05 ^{5C}	38.07 ± 0.63 ^{8B}
	500	0.33 ± 0.01 ^{bA}	0.16 ± 0.01 ^{bb}	0.15 ± 0.01 ^{abA}	0.46 ± 0.00 ^{9C}	0.25 ± 0.02 ^{8C}	87.31 ± 1.30 ^{8B}
Rape straw	600	0.31 ± 0.01 ^{aA}	0.04 ± 0.01 ^{aA}	0.12 ± 0.00 ^{9A}	0.45 ± 0.00 ^{9B}	0.09 ± 0.01 ^{9A}	86.14 ± 1.46 ^{5A}
	CK	3.96 ± 0.35 ^{dA}	1.44 ± 0.08 ^{EB}	0.78 ± 0.08 ^{CA}	0.34 ± 0.00 ^{9A}	3.70 ± 0.11 ^{dA}	–
	300	1.14 ± 0.04 ^{cBC}	0.78 ± 0.00 ^{dB}	0.25 ± 0.05 ^{BA}	0.44 ± 0.00 ^{9C}	4.68 ± 0.16 ^{5C}	–
	400	0.76 ± 0.02 ^{BC}	0.39 ± 0.01 ^{cB}	0.17 ± 0.04 ^{abA}	0.47 ± 0.00 ^{9dB}	2.18 ± 0.02 ^{dD}	49.34 ± 0.89 ^{8C}
Rice straw	500	0.51 ± 0.02 ^{aC}	0.18 ± 0.01 ^{bb}	0.12 ± 0.01 ^{abA}	0.47 ± 0.00 ^{9dD}	0.25 ± 0.00 ^{9C}	80.03 ± 1.78 ^{9A}
	600	0.53 ± 0.02 ^{aC}	0.04 ± 0.01 ^{aA}	0.10 ± 0.00 ^{9A}	0.46 ± 0.00 ^{9C}	0.10 ± 0.00 ^{9B}	88.37 ± 1.20 ^{5A}
	CK	4.42 ± 0.24 ^{eA}	1.29 ± 0.09 ^{EB}	0.80 ± 0.07 ^{9A}	0.35 ± 0.00 ^{9B}	8.62 ± 0.33 ^{5C}	1.33 ± 0.17 ^{8B}
	300	1.31 ± 0.06 ^{dC}	0.78 ± 0.01 ^{dB}	0.29 ± 0.04 ^{CA}	0.43 ± 0.00 ^{9B}	2.14 ± 0.12 ^{dA}	2.02 ± 0.18 ^{9A}
Rice straw	400	0.67 ± 0.03 ^{cBC}	0.31 ± 0.00 ^{CA}	0.20 ± 0.02 ^{CA}	0.44 ± 0.00 ^{9CA}	1.37 ± 0.02 ^{8B}	27.74 ± 1.08 ^{5A}
	500	0.42 ± 0.00 ^{bb}	0.11 ± 0.01 ^{bA}	0.12 ± 0.00 ^{9A}	0.44 ± 0.00 ^{9CA}	0.18 ± 0.00 ^{9B}	82.80 ± 1.90 ^{dAB}
	600	0.36 ± 0.02 ^{ab}	0.03 ± 0.00 ^{9A}	0.08 ± 0.00 ^{9A}	0.44 ± 0.00 ^{9CA}	0.10 ± 0.00 ^{9A}	87.59 ± 2.89 ^{5A}

Different letters a, b, c, and d (A, B, C, and D) in the same column (line) show statistical differences ($p < 0.01$)

and the lowest content of ash. In contrast, the rice straw had the lowest ash content and the highest C content.

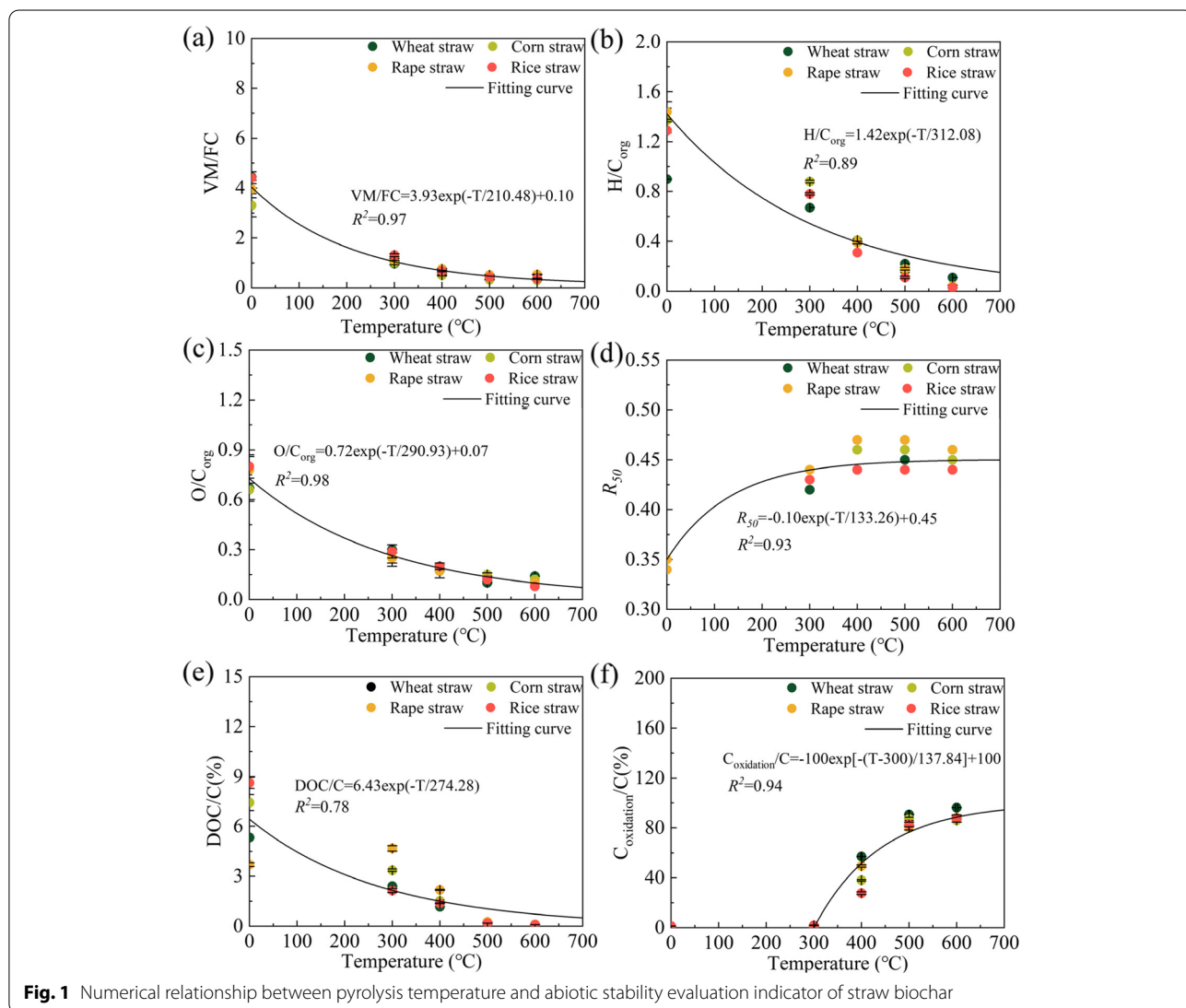
The pyrolysis temperature had a similar effect on the composition and carbon fraction of different straw biochars. As the pyrolysis temperature increased, the content of H, O and VM significantly decreased ($p < 0.01$) and the content of FC and ash increased. The content of C and $C_{\text{oxidation}}$ significantly increased ($p < 0.01$) and the C_{org} content increased with increases in temperature, but the DOC content significantly decreased ($p < 0.01$). At 500–600 °C, the FC, VM and DOC content became steady ($p \geq 0.01$), probably due to the lignocellulosic components' decomposition and volatilization at this temperature range (Zhang et al. 2020). Significant differences were found among the content of ash, C and $C_{\text{oxidation}}$ of different straw biochars ($p < 0.01$). At the same pyrolysis temperature, rice straw biochar showed the lowest ash content and the highest C content, which

may be related to the content of intrinsic compositions in rice straw (Table 1). The content of $C_{\text{oxidation}}$ in wheat straw biochar was much higher than that in other straw biochars.

Therefore, compared with feedstock, pyrolysis temperature may have a more important effect on compositions and carbon fractions of straw biochar, as verified by the results of Fourier transform infrared spectroscopy of straw biochars (Zhang et al. 2020).

3.2 Effects of pyrolysis temperature on biochar abiotic stability

The results of the abiotic stability evaluation indicators of straw biochar derived at different pyrolysis temperatures are shown in Table 2. It can be seen from Table 2 that the pyrolysis temperature had a significant effect on the abiotic stability evaluation indicators of straw biochar ($p < 0.01$). With the increase of pyrolysis temperature,



VM/FC, H/C_{org} , O/C_{org} and DOC/C ratios decreased, however, R_{50} and $C_{oxidation}/C$ ratio increased. Although there were differences among the compositions and carbon fractions of different straw feedstocks, the results of the abiotic stability evaluation indicators were similar among different straw biochars above 500°C. Especially for H/C_{org} , O/C_{org} and DOC/C ratios, there was no significant difference among different straw biochars ($p \geq 0.01$). This indicated that pyrolysis temperature is the main factor affecting the abiotic stability of straw biochars.

The fitting results of the abiotic stability of straw biochars prepared at different pyrolysis temperatures are shown in Fig. 1. As can be seen in Fig. 1, all abiotic stability evaluation indicators increased exponentially with the increasing temperature. However, different stability evaluation indicators showed different exponential function changes, which can be expressed as following formulas:

$$O/C_{org} = -0.72 \exp(-T/290.93) + 0.07 \quad R^2 = 0.97$$

$$H/C_{org} = 1.42 \exp(-T/312.08) \quad R^2 = 0.89$$

$$R_{50} = -0.10 \exp(-T/133.26) + 0.45 \quad R^2 = 0.93$$

$$DOC/C = 6.43 \exp(-T/274.28) \quad R^2 = 0.78$$

$$C_{oxidation}/C = -100 \exp[(300 - T)/137.84] + 100 \quad R^2 = 0.78$$

As depicted in Fig. 1 (a, b, and c), the VM/FC, H/C_{org} and O/C_{org} ratios exponentially decreased as the pyrolysis temperature increased and became steady over 500°C. This might due to the breakage of weaker chemical bonds in feedstock at low temperatures (Imam and Capareda 2012), leading to the depolymerization of lignocellulose. However, the R_{50} exponentially increased as pyrolysis temperature increased from 300 to 500°C, and reached the maximum value at 500°C (Wang et al. 2021b). Straw biochar derived at 500 and 600°C had the similar R_{50} value, which was consistent with the change rule of corrected TPO curves measured (Fig. 2).

The pyrolysis temperature had an obvious exponential function relationship with DOC/C ratio (Fig. 1e). When the pyrolysis temperature was higher than 500°C, the DOC/C ratio was close to zero.

The straw and biochar samples at 300°C had no chemical oxidation-resistance, indicating that the stable C structure may have not formed. When the pyrolysis temperature exceeded 300°C, the $C_{oxidation}/C$ ratio had an exponential function relationship with the pyrolysis

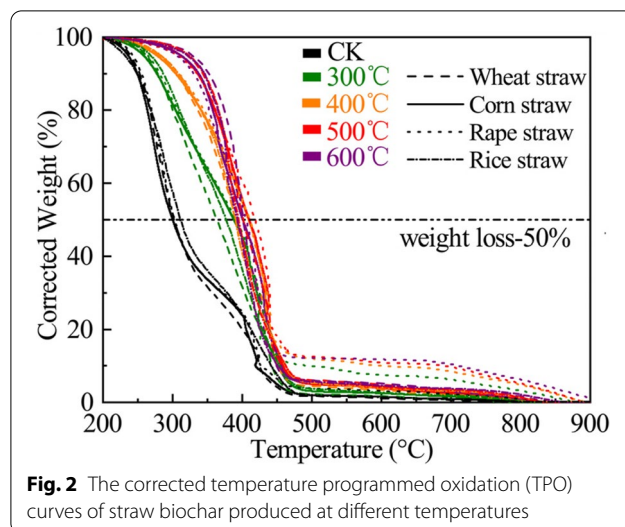


Fig. 2 The corrected temperature programmed oxidation (TPO) curves of straw biochar produced at different temperatures

temperature. With the increase in the pyrolysis temperature, the chemical oxidation-resistant stability increased, which was consistent with the results of previous study (Chen et al. 2016). The $C_{oxidation}/C$ ratio gradually stabilized over 500°C, which might due to the disappearance of unstable components (aliphatic containing C and H, alkane groups) and the formation of chemical oxidation-resistant C structures which were not easily oxidized by chemical reagents (Han et al. 2018; Zhang et al. 2020).

The above results showed that the pyrolysis temperature was an important factor affecting the abiotic stability of straw biochar. The higher the pyrolysis temperature is, the better the abiotic stability of straw biochar is. The abiotic stability of straw biochar tended to be steady over 500°C.

3.3 Correlations among composition, carbon fraction and abiotic stability evaluation indicator of straw biochar

3.3.1 Kendall correlation analysis and factor analysis

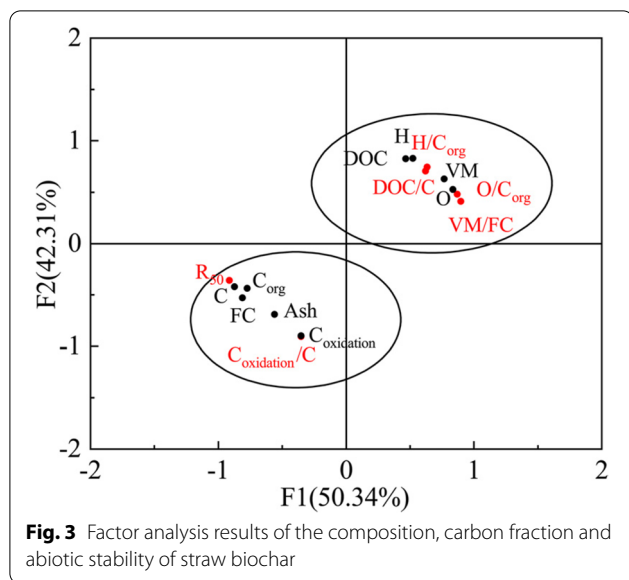
The correlation analysis showed that the composition, carbon fraction and abiotic stability of straw biochar were significantly correlated with the pyrolysis temperature ($p < 0.01$), but had no significant correlations with the types of feedstocks ($p \geq 0.01$) (Table 3). This was consistent with the analysis results in 3.1 and 3.2. Furthermore, there were significant correlations among different stability evaluation indicators ($p < 0.01$).

For further analysis, factor analysis was performed based on the varimax-rotation method (Fig. 3). All characteristics of straw biochars can be divided into two groups. The first group was H, O, VM, DOC, H/C_{org} , O/C_{org} , DOC/C, and VM/FC, and the

Table 3 The Kendall correlation analysis results of the pyrolysis temperature, feedstock, composition, carbon fraction and abiotic stability evaluation indicator of straw biochar

	Pyrolysis temperature	Feedstock Type	C	H	O	FC	VM	Ash	C _{org}	DOC	C _{oxidation}	R ₅₀	VM/FC	H/C _{org}	O/C _{org}	DOC/C	C _{oxidation} /C
Pyrolysis temperature		1.00	0.00	0.00	0.00	0.00	0.00	0.00	0.00	0.00	0.00	0.00	0.00	0.00	0.00	0.00	0.00
Feedstock Type	0.00		0.16	0.71	0.69	0.33	0.79	0.28	0.64	0.95	0.50	0.97	0.59	0.71	0.87	0.95	0.69
C	0.69	-0.25		0.00	0.00	0.00	0.00	0.01	0.00	0.00	0.00	0.00	0.00	0.00	0.00	0.00	0.00
H	-0.90	-0.07	-0.57		0.00	0.00	0.00	0.00	0.00	0.00	0.00	0.00	0.00	0.00	0.00	0.00	0.00
O	-0.85	-0.07	-0.60	0.73		0.00	0.00	0.00	0.00	0.00	0.00	0.00	0.00	0.00	0.00	0.00	0.00
FC	0.71	-0.17	0.61	-0.59	-0.58		0.00	0.01	0.00	0.00	0.00	0.00	0.00	0.00	0.00	0.00	0.00
VM	-0.88	0.05	-0.57	0.80	0.78	-0.76		0.00	0.00	0.00	0.00	0.00	0.00	0.00	0.00	0.00	0.00
Ash	0.73	0.19	0.40	-0.74	-0.70	0.42	-0.66		0.03	0.00	0.00	0.03	0.00	0.00	0.00	0.00	0.00
C _{org}	0.83	-0.08	0.70	-0.51	-0.53	0.58	-0.52	0.35		0.00	0.00	0.00	0.00	0.00	0.00	0.00	0.01
DOC	-0.88	0.01	-0.58	0.82	0.74	-0.63	0.78	-0.68	-0.47		0.00	0.01	0.00	0.00	0.00	0.00	0.00
C _{oxidation}	0.83	-0.12	0.61	-0.72	-0.71	0.62	-0.76	0.66	0.50	-0.76		0.00	0.00	0.00	0.00	0.00	0.00
R ₅₀	0.62	-0.01	0.65	-0.49	-0.57	0.63	-0.53	0.38	0.77	-0.43	0.56		0.00	0.00	0.00	0.01	0.00
VM/FC	-0.83	0.09	-0.58	0.70	0.73	-0.85	0.91	-0.57	-0.53	0.76	-0.71	-0.54		0.00	0.00	0.00	0.00
H/C _{org}	-0.92	-0.07	-0.58	0.97	0.76	-0.62	0.82	-0.75	-0.56	0.82	-0.74	-0.52	0.73		0.00	0.00	0.00
O/C _{org}	-0.87	-0.03	-0.67	0.75	0.92	-0.60	0.77	-0.67	-0.61	0.75	-0.71	-0.60	0.72	0.79		0.00	0.00
DOC/C	-0.90	0.01	-0.61	0.84	0.76	-0.65	0.79	-0.68	-0.50	0.97	-0.76	-0.46	0.78	0.83	0.76		0.00
C _{oxidation} /C	0.82	-0.07	0.56	-0.73	-0.72	0.59	-0.77	0.67	0.45	-0.76	0.95	0.53	-0.67	-0.75	-0.71	-0.75	

The lower left part of the table is the correlation coefficient R, and the upper right part is the significance test result p



second group was C, FC, C_{org} , $C_{oxidation}$, ash, R_{50} and $C_{oxidation}/C$. Within the same group, there was a positive relationship between any two characteristics. And there was a negative correlation between any two characteristics from different groups. Except for R_{50} , the rest of thermal stability evaluation indicators were clustered into the same group with dissolution stability evaluation indicators, and the others including R_{50} were clustered into another group. This indicated the close relationship among H/C_{org} , O/C_{org} , DOC/C , and VM/FC , as well as R_{50} and $C_{oxidation}/C$. Thus, it is necessary to further study the quantitative relationships among different abiotic stability evaluation indicators of straw biochar.

3.3.2 Quantitative relationships of abiotic stability evaluation indicators of straw biochar

The linear correlations among different abiotic stability evaluation indicators of straw biochar are shown in Fig. 4. The significance of model test was 0.000, indicating that the results of fitting analysis were effective. The linearity of different abiotic stability evaluation indicators varied.

Among the evaluation indicators of thermal stability, VM/FC and R_{50} , O/C_{org} and R_{50} , as well as VM/FC and O/C_{org} , showed a strong linear relationship ($R^2 > 0.90$). Therefore, VM/FC , O/C_{org} and R_{50} can replace each other in evaluating the thermal stability of biochar. In addition, there was a high linear relationship between H/C_{org} and O/C_{org} ($R^2 = 0.81$), which may be related to the high linear relationship between H and O in straw biochar ($R^2 = 0.83$) (Zhang et al. 2020). There was a high correlation between H/C_{org} and DOC/C ($R^2 = 0.81$) (Fig. 4b).

Both VM/FC and O/C_{org} showed a linear correlation with DOC/C ($R^2 = 0.74$ and $R^2 = 0.77$, respectively). There was no linear relationship between the indicators of dissolution stability and chemical oxidation-resistant stability, indicating that there were differences between them. In Fig. 4c, $C_{oxidation}/C$ showed a high linear correlation with H/C_{org} ($R^2 = 0.81$). It is suggested that H/C_{org} can be selected as an alternative evaluation indicator for the evaluation of dissolution stability and chemical oxidation-resistant stability. In view of these results, it can be considered that the thermal stability evaluation indicators, especially H/C_{org} , are of great significance for the evaluation of abiotic stability.

3.3.3 Multivariate analysis of composition, carbon fraction and abiotic stability of straw biochar

A multivariate analysis of the composition, carbon fraction and abiotic stability of straw biochar is needed to simplify the evaluation of abiotic stability for practical application. The results of binary linear regression analysis are shown in Fig. 5. Both VM/FC and DOC/C were affected by the interactive effects of H and O. Comparing with DOC/C . There was a better binary linear relationship among VM/FC , H and O, which indicated that the VM/FC ratio could be calculated by H and O content. C, C_{org} , and FC were respectively selected to fit R_{50} with ash. Compared with FC and C_{org} , there was a better fitting effect of C and ash on R_{50} ($R^2 = 0.90$), which demonstrated that the content of C and ash can be used for evaluating R_{50} . And compared with R_{50} , there were worse results when $C_{oxidation}/C$ was fitted with C and ash, C_{org} and ash, as well as FC and ash. This demonstrated that chemical oxidation-resistant stability may be affected by other factors, in addition to these interactions.

4 Conclusion

It can be concluded that pyrolysis temperature influenced the compositions and carbon fractions directly, which affected the abiotic stability of biochar ($p < 0.01$). The higher the pyrolysis temperature (up to 500 °C), the higher the abiotic stability of biochar.

The exponential functions of stability indicators with pyrolysis temperature are as follows:

$$O/C_{org} = -0.72 \exp(-T/290.93) + 0.07 \quad R^2 = 0.97$$

$$H/C_{org} = 1.42 \exp(-T/312.08) \quad R^2 = 0.89$$

$$R_{50} = -0.10 \exp(-T/133.26) + 0.45 \quad R^2 = 0.93$$

$$DOC/C = 6.43 \exp(-T/274.28) \quad R^2 = 0.78$$

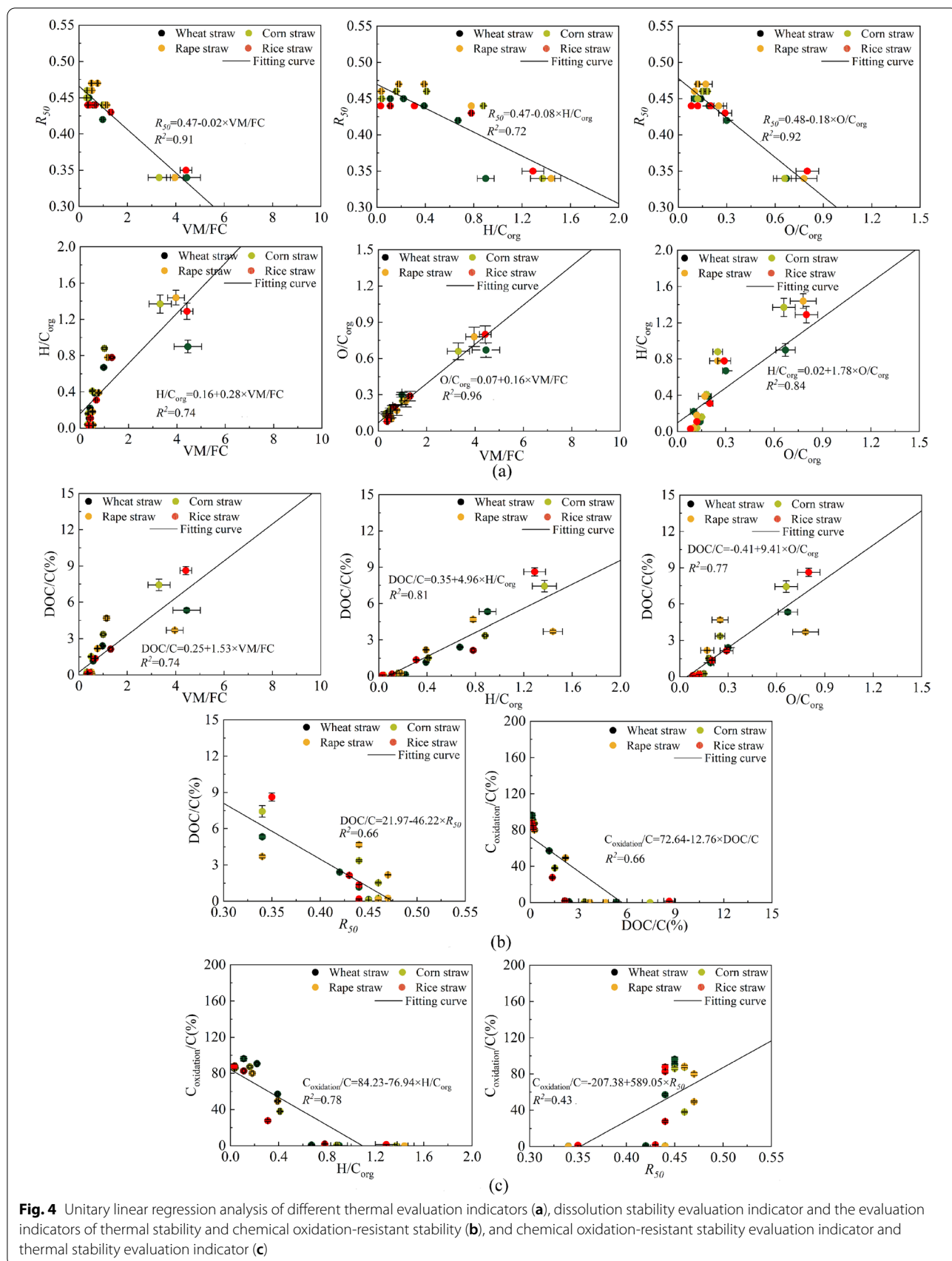


Fig. 4 Unitary linear regression analysis of different thermal evaluation indicators (a), dissolution stability evaluation indicator and the evaluation indicators of thermal stability and chemical oxidation-resistant stability (b), and chemical oxidation-resistant stability evaluation indicator and thermal stability evaluation indicator (c)

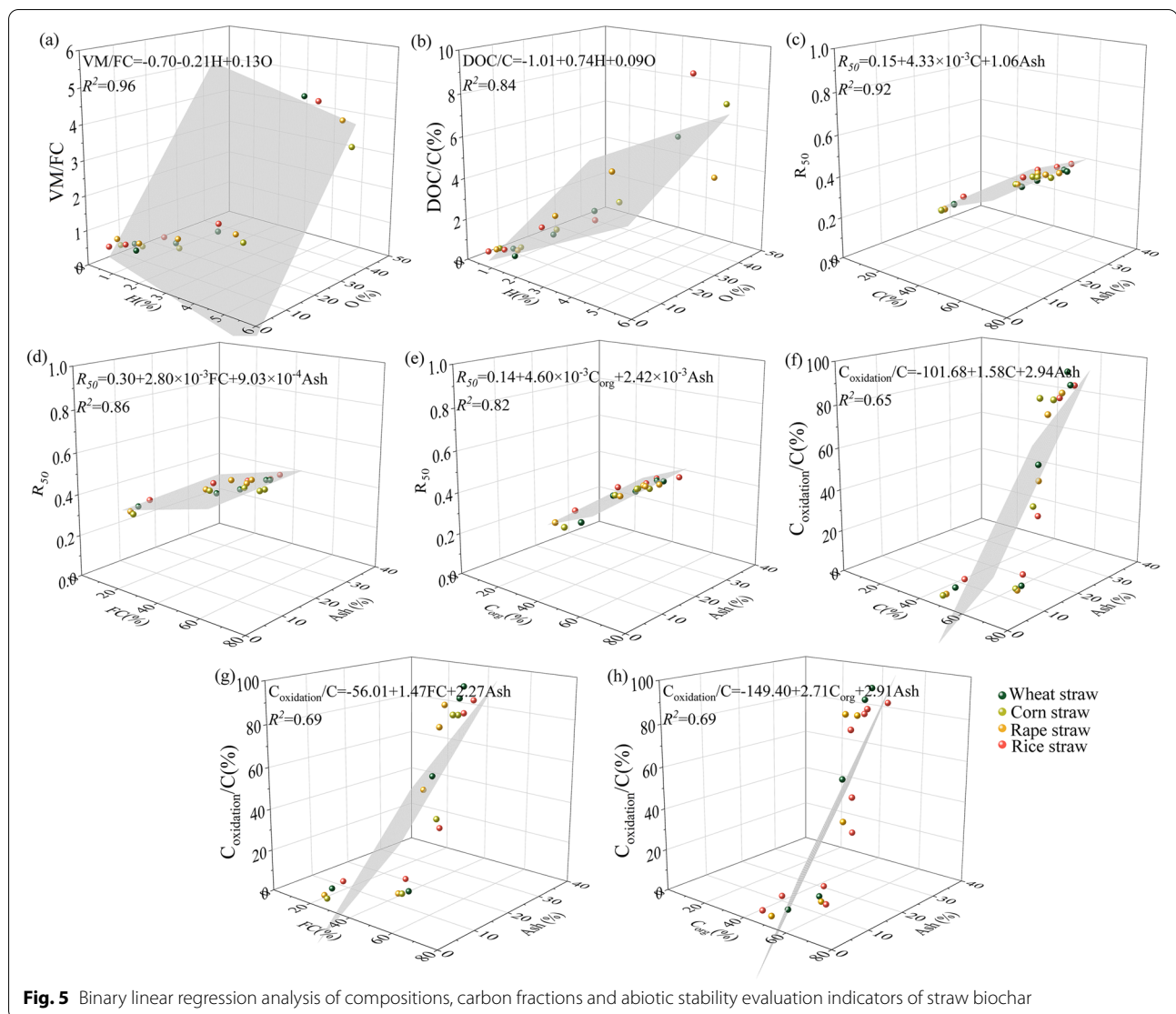


Fig. 5 Binary linear regression analysis of compositions, carbon fractions and abiotic stability evaluation indicators of straw biochar

$$C_{oxidation}/C = -100 \exp [(300 - T)/137.84] + 100 \quad R^2 = 0.78$$

The established unitary and binary linear regressions equations among compositions, carbon fractions and the abiotic stability indicators are valuable for simplifying the screening of appropriate indicators for evaluating the properties and abiotic stability of biochar, which will be beneficial to the effective utilization of straw biochar, especially in the scope of carbon capturing and sequestering application.

Acknowledgements

The authors are grateful for the financial support of the earmarked fund for CARS (CARS-36) and Innovative Research Team in University of Education Ministry of China (IRT_17R105).

Authors' contributions

Conceptualization: Lujia Han; Investigation: Xiaoxiao Zhang, Xueqi Yang; Methodology: Xiaoxiao Zhang, Sicong Tian, Hehu Zhang; Formal analysis and data

curation: Xiaoxiao Zhang, Xinlei Wang; Validation: Xueqi Yang, Xinlei Wang, Hehu Zhang; Writing – original draft: Xiaoxiao Zhang; Writing – review and editing: Xiangru Yuan, Sicong Tian, Lujia Han. The author(s) read and approved the final manuscript.

Funding

The study was funded by China Agriculture Research System (CARS-36) and Innovative Research Team in University of Education Ministry of China (IRT_17R105).

Availability of data and materials

The datasets generated during the current study are available from the corresponding author on reasonable request.

Declarations

Competing interests

The authors declare that they have no known competing financial interests or personal relationships that could have appeared to influence the work reported in this manuscript.

Received: 11 May 2022 Accepted: 11 August 2022
Published online: 29 August 2022

References

- Aller D, Bakshi S, Laird DA (2017) Modified method for proximate analysis of biochars. *J Anal Appl Pyrolysis* 124:335–342. <https://doi.org/10.1016/j.jaap.2017.01.012>
- Ameloot N, Graber ER, Verheijen FGA, De Neve S (2013) Interactions between biochar stability and soil organisms: review and research needs. *Eur J Soil Sci* 64(4):379–390. <https://doi.org/10.1111/ejss.12064>
- Calvelo-Pereira R, Kaal J, Camps Arbustain M, Pardo Lorenzo R, Aitkenhead W, Hedley M, Macias F, Hindmarsh J, Macia-Agullo JA (2011) Contribution to characterisation of biochar to estimate the labile fraction of carbon. *Org Geochem* 42(11):1331–1342. <https://doi.org/10.1016/j.orggeochem.2011.09.002>
- Chen D, Yu X, Song C, Pang X, Huang J, Li Y (2016) Effect of pyrolysis temperature on the chemical oxidation stability of bamboo biochar. *Bioresour Technol* 218:1303–1306. <https://doi.org/10.1016/j.biortech.2016.07.112>
- Crombie K, Mašek O, Sohi SP, Brownsort P, Cross A (2013) The effect of pyrolysis conditions on biochar stability as determined by three methods. *Glob Change Biol Bioenergy* 5(2):122–131. <https://doi.org/10.1111/gcbb.12030>
- Das SK, Ghosh GK, Avasthe RK, Sinha K (2021) Compositional heterogeneity of different biochar: effect of pyrolysis temperature and feedstocks. *J Environ Manage* 278:111501. <https://doi.org/10.1016/j.jenvman.2020.11.1501>
- De la Rosa JM, Rosado M, Paneque M, Miller AZ, Knicker H (2018) Effects of aging under field conditions on biochar structure and composition: implications for biochar stability in soils. *Sci Total Environ* 613–614:969–976. <https://doi.org/10.1016/j.scitotenv.2017.09.124>
- Enders A, Hanley K, Whitman T, Joseph S, Lehmann J (2012) Characterization of biochars to evaluate recalcitrance and agronomic performance. *Bioresour Technol* 114:644–653. <https://doi.org/10.1016/j.biortech.2012.03.022>
- Gómez N, Rosas JG, Singh S, Ross AB, Sánchez ME, Cara J (2016) Development of a gained stability index for describing biochar stability: relation of high recalcitrance index (R50) with accelerated ageing tests. *J Anal Appl Pyrolysis* 120:37–44. <https://doi.org/10.1016/j.jaap.2016.04.007>
- Han L, Ro KS, Wang Y, Sun K, Sun H, Libra JA, Xing B (2018) Oxidation resistance of biochars as a function of feedstock and pyrolysis condition. *Sci Total Environ* 616–617:335–344. <https://doi.org/10.1016/j.scitotenv.2017.11.014>
- Han L, Sun K, Yang Y, Xia X, Li F, Yang Z, Xing B (2020) Biochar's stability and effect on the content, composition and turnover of soil organic carbon. *Geoderma* 364:114184. <https://doi.org/10.1016/j.geoderma.2020.114184>
- Harvey OR, Kuo L, Zimmerman AR, Louchouart P, Amonette JE, Herbert BE (2012) An index-based approach to assessing recalcitrance and soil carbon sequestration potential of engineered black carbons (biochars). *Environ Sci Technol* 46(3):1415–1421. <https://doi.org/10.1021/es2040398>
- Hassan M, Liu Y, Naidu R, Parikh SJ, Du J, Qi F, Willett IR (2020) Influences of feedstock sources and pyrolysis temperature on the properties of biochar and functionality as adsorbents: a meta-analysis. *Sci Total Environ* 744:140714. <https://doi.org/10.1016/j.scitotenv.2020.140714>
- Hepburn C, Adlen E, Beddington J, Carter EA, Fuss S, Mac Dowell N, Minx JC, Smith P, Williams CK (2019) The technological and economic prospects for CO₂ utilization and removal. *Nature* 575(7781):87–97. <https://doi.org/10.1038/s41586-019-1681-6>
- Imam T, Capareda S (2012) Characterization of bio-oil, syn-gas and bio-char from switchgrass pyrolysis at various temperatures. *J Anal Appl Pyrolysis* 93:170–177. <https://doi.org/10.1016/j.jaap.2011.11.010>
- Jaffe R, Ding Y, Niggemann J, Vahatalo AV, Stubbins A, Spencer RGM, Campbell J, Dittmar T (2013) Global charcoal mobilization from soils via dissolution and riverine transport to the oceans. *Sci (Am Assoc Adv Sci)* 340(6130):345–347. <https://doi.org/10.1126/science.1231476>
- Jing F, Sun Y, Liu Y, Wan Z, Chen J, Tsang D (2022) Interactions between biochar and clay minerals in changing biochar carbon stability. *Sci Total Environ* 809:151124. <https://doi.org/10.1016/j.scitotenv.2021.151124>
- Kim H, Kim J, Kim T, Alessi DS, Baek K (2021) Interaction of biochar stability and abiotic aging: influences of pyrolysis reaction medium and temperature. *Chem Eng* 41:1:128441. <https://doi.org/10.1016/j.cej.2021.128441>
- Kim J, Oh S, Park Y (2020) Overview of biochar production from preservative-treated wood with detailed analysis of biochar characteristics, heavy metals behaviors, and their ecotoxicity. *J Hazard Mater* 384:121356. <https://doi.org/10.1016/j.jhazmat.2019.121356>
- Lehmann J (2007) A handful of carbon. *Nature* 447(7141):143–144. <https://doi.org/10.1038/447143a>
- Leng L, Huang H (2018) An overview of the effect of pyrolysis process parameters on biochar stability. *Bioresour Technol* 270:627–642. <https://doi.org/10.1016/j.biortech.2018.09.030>
- Leng L, Huang H, Li H, Li J, Zhou W (2019) Biochar stability assessment methods: a review. *Sci Total Environ* 647:210–222. <https://doi.org/10.1016/j.scitotenv.2018.07.402>
- Lian F, Xing B (2017) Black carbon (biochar) in water/soil environments: molecular structure, sorption, stability, and potential risk. *Environ Sci Technol* 51(23):13517–13532. <https://doi.org/10.1021/acs.est.7b02528>
- Liu B, Liu Q, Wang X, Bei Q, Zhang Y, Lin Z, Liu G, Zhu J, Hu T, Jin H, Wang H, Sun X, Lin X, Xie Z (2020a) A fast chemical oxidation method for predicting the long-term mineralization of biochar in soils. *Sci Total Environ* 718:137390. <https://doi.org/10.1016/j.scitotenv.2020.137390>
- Liu G, Pan X, Ma X, Xin S, Xin Y (2020b) Effects of feedstock and inherent mineral components on oxidation resistance of biochars. *Sci Total Environ* 726:138672. <https://doi.org/10.1016/j.scitotenv.2020.138672>
- Liu Y, Chen J (2022) Effect of ageing on biochar properties and pollutant management. *Chemosphere* 292:133427. <https://doi.org/10.1016/j.chemosphere.2021.133427>
- Pariyar P, Kumari K, Jain MK, Jadhao PS (2020) Evaluation of change in biochar properties derived from different feedstock and pyrolysis temperature for environmental and agricultural application. *Sci Total Environ* 713:136433. <https://doi.org/10.1016/j.scitotenv.2019.136433>
- Paustian K, Lehmann J, Ogle S, Reay D, Robertson GP, Smith P (2016) Climate-smart soils. *Nature* 532(7597):49–57. <https://doi.org/10.1038/nature17174>
- Qian K, Kumar A, Zhang H, Bellmer D, Huhnke R (2015) Recent advances in utilization of biochar. *Renew Sustain Energy Rev* 42:1055–1064. <https://doi.org/10.1016/j.rser.2014.10.074>
- Quan G, Fan Q, Zimmerman AR, Sun J, Cui L, Wang H, Gao B, Yan J (2020) Effects of laboratory biotic aging on the characteristics of biochar and its water-soluble organic products. *J Hazard Mater* 382:121071. <https://doi.org/10.1016/j.jhazmat.2019.121071>
- Singh G, Lakhi KS, Sil S, Bhosale SV, Kim I, Albahily K, Vinu A (2019) Biomass derived porous carbon for CO₂ capture. *Carbon* 148:164–186. <https://doi.org/10.1016/j.carbon.2019.03.050>
- Sohi SP (2012) Carbon storage with benefits. *Science* 338(6110):1034–1035. <https://doi.org/10.1126/science.1225987>
- Wang H, Nan Q, Waqas M, Wu W (2022) Stability of biochar in mineral soils: assessment methods, influencing factors and potential problems. *Sci Total Environ* 806:150789. <https://doi.org/10.1016/j.scitotenv.2021.150789>
- Wang J, Shi L, Zhai L, Zhang H, Wang S, Zou J, Shen Z, Lian C, Chen Y (2021a) Analysis of the long-term effectiveness of biochar immobilization remediation on heavy metal contaminated soil and the potential environmental factors weakening the remediation effect: a review. *Ecotoxi Environ Safe* 207:111261. <https://doi.org/10.1016/j.ecoenv.2020.111261>
- Wang R, Gibson CD, Berry TD, Jiang Y, Bird JA, Filley TR (2017) Photooxidation of pyrogenic organic matter reduces its reactive, labile C pool and the apparent soil oxidative microbial enzyme response. *Geoderma* 293:10–18. <https://doi.org/10.1016/j.geoderma.2017.01.011>
- Wang W, Bai J, Lu Q, Zhang G, Wang D, Jia J, Guan Y, Yu L (2021b) Pyrolysis temperature and feedstock alter the functional groups and carbon sequestration potential of *Phragmites australis*- and *Spartina alterniflora*-derived biochars. *Glob Change Biol Bioenergy* 13(3):493–506. <https://doi.org/10.1111/gcbb.12795>
- Wei S, Zhu M, Fan X, Song J, Peng P, Li K, Jia W, Song H (2019) Influence of pyrolysis temperature and feedstock on carbon fractions of biochar produced from pyrolysis of rice straw, pine wood, pig manure and sewage sludge. *Chemosphere* 218:624–631. <https://doi.org/10.1016/j.chemosphere.2018.11.177>
- Woolf D, Amonette JE, Street-Perrott FA, Lehmann J, Joseph S (2010) Sustainable biochar to mitigate global climate change. *Nat Commun* 1(1). <https://doi.org/10.1038/ncomms1053>
- Wu H, Qi Y, Dong L, Zhao X, Liu H (2019) Revealing the impact of pyrolysis temperature on dissolved organic matter released from the biochar prepared from *Typha orientalis*. *Chemosphere* 228:264–270. <https://doi.org/10.1016/j.chemosphere.2019.04.143>
- Wu L, Ni J, Zhang H, Yu S, Wei R, Qian W, Chen W, Qi Z (2022) The composition, energy, and carbon stability characteristics of biochars derived from thermo-conversion of biomass in air-limitation, CO₂, and N₂ at different temperatures. *Waste Manag* 141:136–146. <https://doi.org/10.1016/j.wasman.2022.01.038>

- Xu Z, He M, Xu X, Cao X, Tsang DCW (2021) Impacts of different activation processes on the carbon stability of biochar for oxidation resistance. *Bioresour Technol* 338:125555. <https://doi.org/10.1016/j.biortech.2021.125555>
- Yang F, Xu Z, Yu L, Gao B, Xu X, Zhao L, Cao X (2018) Kaolinite Enhances the Stability of the Dissolvable and Undissolvable Fractions of Biochar via Different Mechanisms. *Environ Sci Technol* 52(15): 8321–8329. <https://doi.org/10.1021/acs.est.8b00306>
- Yu Z, Ling L, Singh BP, Luo Y, Xu J (2020) Gain in carbon: deciphering the abiotic and biotic mechanisms of biochar-induced negative priming effects in contrasting soils. *Sci Total Environ* 746:141057. <https://doi.org/10.1016/j.scitotenv.2020.141057>
- Zhang P, Li Y, Cao Y, Han L (2019) Characteristics of tetracycline adsorption by cow manure biochar prepared at different pyrolysis temperatures. *Bioresour Technol* 285:121348. <https://doi.org/10.1016/j.biortech.2019.121348>
- Zhang X, Zhang P, Yuan X, Li Y, Han L (2020) Effect of pyrolysis temperature and correlation analysis on the yield and physicochemical properties of crop residue biochar. *Bioresour Technol* 296:122318. <https://doi.org/10.1016/j.biortech.2019.122318>
- Zornoza R, Moreno-Barriga F, Acosta JA, Muñoz MA, Faz A (2016) Stability, nutrient availability and hydrophobicity of biochars derived from manure, crop residues, and municipal solid waste for their use as soil amendments. *Chemosphere* 144:122–130. <https://doi.org/10.1016/j.chemosphere.2015.08.046>

Publisher's Note

Springer Nature remains neutral with regard to jurisdictional claims in published maps and institutional affiliations.